JOURNAL OF AIRCRAFT
Vol. 46, No. 5, September–October 2009

Flow past a Yawed Rectangular Cavity in Transonic and Low Supersonic Flows

B. H. K. Lee*
B. H. K. Lee Consulting, Ottawa, Ontario K1V 9B1, Canada
and
D. M. Orchard† and F. C. Tang‡
National Research Council, Ottawa, Ontario K1A 0R6, Canada

DOI: 10.2514/1.40729

The effect of yaw on the steady and unsteady pressure measurements along the floor and walls of a rectangular cavity with a length-to-depth ratio of 5 was investigated. Statistical analyses were carried out on the pressure outputs to determine modal frequencies, amplitudes, and phase relationships. Rossiter's empirical formula was found to give good estimates of the frequencies of the acoustic tones for moderate yaw angles up to 20 deg, which was the highest value tested. The dominant acoustic mode was a function of the yaw angle, and it switched over to a higher mode when the yaw angle exceeded a critical value. At $M = 0.84$ and $M = 1.11$, the aft wall pressure distributions and acoustic mode amplitudes showed a very different behavior with changes in yaw angle for transonic and supersonic Mach numbers.

Nomenclature

C_p = pressure coefficient
D = cavity depth
f = frequency
k = constant
L = cavity length
M = freestream Mach number
n = mode number
p = pressure
St = Strouhal number
U = freestream velocity
W = cavity span
α = constant
ψ = yaw angle

I. Introduction

STORES carriage inside an internal weapons bay can reduce drag, enhance maneuverability, and minimize the radar cross section of military combat aircraft. However, the flowfield associated with a cavity presents a number of challenges for the safe carriage and release of stores. The large nose-up pitching moments experienced by stores on traversing the pressure gradients inside the cavity may endanger the parent aircraft because of the possibility of collision when stores are released. In addition, the unsteady flow can generate self-sustained oscillations as a result of shear layer instability and acoustic tone coupling. The intense sound field that is produced can exceed 170 dB. The structural integrity of stores, as well as the aircraft, is a matter of concern, and numerous investigations have been reported in the past two decades. The studies are mainly concentrated in three areas: experimental, theoretical and semi-empirical, and computational fluid dynamics (CFD) (Reynolds-averaged Navier–Stokes, large-eddy simulation, direct numerical simulation, etc.). Review articles on these subjects are given by Komerath et al. [1], Chokani [2] and Grace [3].

Most of the investigations have been carried out on rectangular cavities at zero yaw angle, and the parameters investigated are Mach number, Reynolds number, cavity length L, depth D, and span W ratios. A CFD study of the steady flowfield inside a yawed cavity has been reported by Baysal and Yen [4] for supersonic flows at a yaw angle $\psi = 45$ deg. They showed that the flow is dominated by a large vortex that grows in size from the separating side wall to the impinged side wall. The vortex rotates in both the vertical and horizontal planes. The separation and reattachment lines on the floor display a more complex topology than the unyawed cavity. Windtunnel studies have been conducted at the Langley 0.3-Meter Transonic Cryogenic Tunnel on a rectangular cavity at $\psi = 15$ deg. Plentovich et al. [5] give static results of the pressure distributions along the longitudinal centerline of cavities with various L/D ratios showing the effects of Mach number and Reynolds number. Unsteady results showing the mode shapes for $\psi = 0$ and 15 deg are given by Tracy and Plentovich [6].

At moderate yaw angles, the frequency of the acoustic tones generated inside the cavity can be predicted quite accurately using Rossiter's [7] empirical formula. Rossiter's vortex model [7] has been shown by Bilanin and Covert [8] and later by Tam and Block [9] to give similar results as the Heller and Bliss [10] oscillating shear layer model.

In Rossiter's [7] model, the degree of vorticity concentration, and hence circulation of the vortex that impinges on the cavity aft wall, is a function of the cavity length L. For an unyawed cavity with a sufficiently large L/D ratio, so that the shear layer has gone through the stages of linear growth, instability, nonlinear saturation, and finally coherent or large structure formation, Rossiter [7] provided a satisfactory model that synchronizes the vortices and acoustic waves to form a coupled system. However, in the case of the yawed cavity when the shear layer from the separating sidewall has not developed sufficiently to generate vortices, the Heller and Bliss [10] model gives the possible mechanisms of the generation of the longitudinal acoustic waves. It should be noted that the acoustic waves will be weakened as the yaw angle increases because the shear layer is increasingly less developed.

The present paper presents results showing the effect of yaw on the cavity floor and wall pressure distributions. The acoustic modes are identified from statistical analysis and the yaw angle at which the

Presented as Paper 6234 at the 26th Applied Aerodynamics Conference, Honolulu, HI, 18–21 August 2008; received 1 September 2008; revision received 27 May 2009; accepted for publication 29 May 2009.

*Also adjunct Professor, Department of Mechanical Engineering, University of Ottawa, Ottawa, Ontario, Canada; bhk_lee@yahoo.com. Associate Fellow AIAA (Corresponding Author).
†Research Officer, Institute for Aerospace Research, Wind-Tunnel Group.
‡Senior Research Officer, Institute for Aerospace Research, Aerodynamics Laboratory. Member AIAA.

dominant mode switches to a higher mode is determined. Phase relationships of the longitudinal standing waves inside the cavity as a function of the yaw angle are also measured. The investigation was carried out at $M = 0.84$ and $M = 1.11$ to show the effect of transonic and low supersonic Mach numbers on the cavity resonance behavior.

II. Experimental Setup

The tests were conducted in the 5-inch trisonic wind tunnel at the Institute for Aerospace Research, National Research Council, Canada. This tunnel is a blowdown facility with a Mach number range from 0.1 to 4.0. The tunnel is capable of almost continuous operation but, for the present study, the run time was limited to approximately 5 s. The test assembly consisted of a 13.45 in. boundary-layer development plate which spanned the full width of one side of the working section. When installed, the test plate assembly replaced one of the perforated walls and was held 0.5 in. above the nominal floor position to ensure the test plate was outside of the oncoming boundary layer. Flow was allowed to pass underneath the test plate to ensure test section blockage was kept to a minimum. The cavity was 3.75 in. long, 0.75 in. span, and had its front lip 5.8 in. downstream from the leading edge of the development plate. The length-to-depth L/D and length-to-span L/W ratios of 5 were chosen to coincide with the M219 cavity used in the experimental study of Henshaw [11]. An array of 0.002 in. turbulence trips spaced at 0.1 in. intervals was positioned 1 in. downstream from the leading edge of the plate to promote a turbulent boundary-layer development at the cavity location. The boundary-layer thickness δ at Mach 0.84, obtained from a pitot probe at 0.25 in. upstream of the cavity front lip, was found to be 0.095 in. with a displacement thickness δ^* of 0.016 in. A schematic view of the cavity and the pressure transducers' positions are shown in Fig. 1, and Table 1 gives the coordinates of the locations of the 16 fast-response pressure transducers. The frequency response of the transducers was about 20 kHz and calibration showed a practically flat response up to a test frequency of 6 kHz. Data from all pressure transducers were sampled at 18 kHz for 5 s following low-pass filtering at 6 kHz using an eighth-order Butterworth filter. The low-pass frequency was kept constant because the highest acoustic frequency detected was about 4.5 kHz in the range of Mach numbers tested. The cavity could be yawed on a turntable with a range of $\psi = \pm 25$ deg. In the tests, ψ varied from 0 to 20 deg in increments of 5 deg. During the tests, transducers 2, 3, and 12 were damaged and the results were unreliable and discarded.

The tests were performed at freestream Mach numbers of 0.84 and 1.11 to obtain mean and unsteady pressure distributions. In both cases, total pressure was adjusted to maintain a flow Reynolds number close to 2.75×10^6 per foot. Tunnel settings yielded dynamic pressures, used to normalize all pressure data, of approximately 8.9 psi at Mach 0.84 and 10.8 psi at Mach 1.11. A more detailed description of the facility and test procedures is given by Orchard et al. [12].

III. Pressure Measurements on Cavity Floor

A. Cavity Floor C_p and $C_{p_{\text{rms}}}$

The flow past a yawed rectangular cavity is shown in Fig. 2. Assuming that the streamlines are straight lines unaffected by three-dimensional effects created by the walls, the aft wall is influenced only by the shear layer generated at the separating sidewall when $\psi > \psi_c$. Here, ψ is the yaw angle and the critical yaw angle is given by $\psi_c = \arctan W/L$. The rectangular cavity under investigation has a value of $L/W = 5$ and hence $\psi_c = 11.3$ deg. As ψ increases beyond ψ_c, the portion of the sidewall shear layer that affects the aft wall decreases and is given by the length $ab = W \cot \psi$.

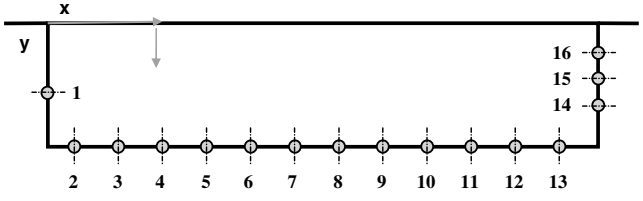

Fig. 1 Location of transducers.

Table 1 Pressure transducer positions

Transducer	x/L	y/D	Location
1	0	0.626	Forward wall
2	0.05	1.0	Cavity floor
3	0.13	1.0	Cavity floor
4	0.21	1.0	Cavity floor
5	0.3	1.0	Cavity floor
6	0.38	1.0	Cavity floor
7	0.46	1.0	Cavity floor
8	0.54	1.0	Cavity floor
9	0.62	1.0	Cavity floor
10	0.7	1.0	Cavity floor
11	0.79	1.0	Cavity floor
12	0.87	1.0	Cavity floor
13	0.95	1.0	Cavity floor
14	1.0	0.752	Aft wall
15	1.0	0.501	Aft wall
16	1.0	0.268	Aft wall

Figures 3 and 4 show the time-averaged pressure coefficient $C_p = (p - p_\infty)/q$ and unsteady pressure expressed as $C_{p_{\text{rms}}} = p_{\text{rms}}/q$ along the cavity floor at $M = 1.11$ and yaw angle ψ from 0 to 20 deg in steps of 5 deg. Here, $q = \rho U^2/2$, where ρ and U are the freestream density and velocity, respectively. The results were deduced from approximately 3.527 s of data from the pressure time series. Note that the pressure at yaw along the centerline of the cavity is skewed to the flow direction.

The C_p distribution with x/L for the flow at $\psi = 0$ deg is of the open cavity type using the definition of the different types of cavity flows given by Plentovich et al. [5]. This is characterized by a positive C_p at the base of the front wall. The pressure remains positive or decreases slightly below zero and, past the midpoint of the cavity length, the pressure increases rapidly toward the aft wall. Plentovich et al. [5] showed that, for an initially open cavity flow at $\psi = 0$ deg, and at high subsonic or transonic Mach numbers, increasing the yaw angle to 15 deg resulted in the flow being of the transitional-open

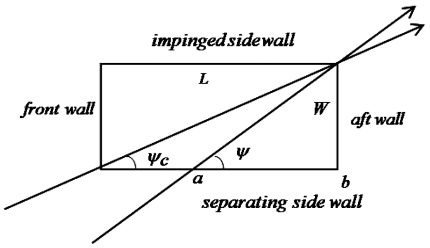

Fig. 2 Schematic of flow past a yawed rectangular cavity.

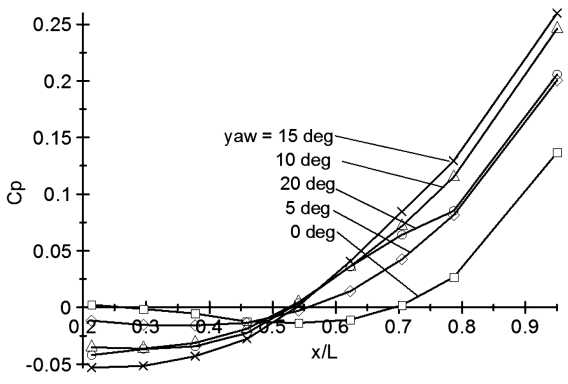

Fig. 3 C_p distribution on cavity floor at $M = 1.11$.

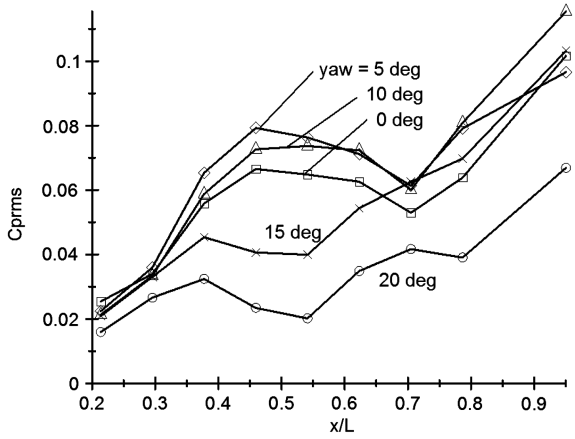

Fig. 4 $C_{p\text{rms}}$ distribution on cavity floor at $M = 1.11$.

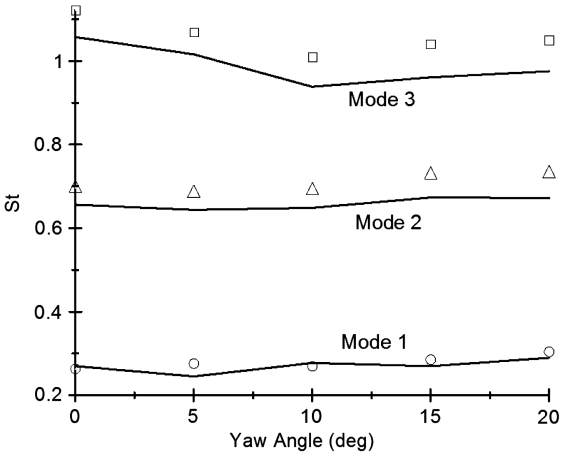

Fig. 5 Frequency versus yaw angle. Solid lines are at $M = 1.11$; symbols are at $M = 0.84$.

type. Typically, this type of flow has a negative pressure distribution along the front portion of the cavity floor and starts to increase to positive values toward the aft wall for x/L about 0.5. The pressure increases more rapidly with x/L than in the case for $\psi = 0$ deg.

For supersonic flows, the results for $\psi = 0$ deg are given in Fig. 3 and they show the flow to be of the transitional-open type using the classification of flows according to Plentovich et al. [5]. The effect of increasing the yaw angle is to decrease the pressure at the front portion of the cavity, while at the aft portion of the cavity, the pressure increases with ψ up to $\psi = 15$ deg. Increasing ψ to 20 deg has the opposite effect where the pressure decreases instead.

The results [13] at $M = 0.84$ are quite similar to those at $M = 1.11$ with the exception that the C_p levels are higher than those at the supersonic Mach number tested. The C_p versus x/L curves for $\psi = 10$ and 15 deg are further apart from those at $M = 1.11$, and the C_p distribution on the cavity floor for $x/L > 0.5$ is also highest at $\psi = 15$ deg.

The $C_{p_{\text{rms}}}$ distribution along the cavity floor at $M = 1.11$ is shown in Fig. 4. The results for $\psi = 0$, 5, and 10 deg are fairly close and $C_{p_{\text{rms}}}$ increases with ψ until, at $\psi = 15$ deg, a large drop is detected for $x/L < 0.7$. Further increase to $\psi = 20$ deg results in even larger decrease in $C_{p_{\text{rms}}}$. The broad peaks observed in the curves are due to the turbulent broadband fluctuations with contributions from the acoustic tones. Similar results [13] are obtained at $M = 0.84$. The main difference is the closeness of the curves at $\psi = 0$, 5, and 10 deg for $x/L < 0.7$ than those at $M = 1.11$.

B. Mode Frequency, Amplitude, and Phase

Statistical analyses were carried out on the instantaneous C_p time series using a fast Fourier transform (FFT) algorithm from LabVIEW. The same 3.527 s of data used in computing time-averaged C_p and unsteady $C_{p_{\text{rms}}}$ was analyzed, and there were 63,488 samples with the sampling frequency set at 18 kHz. A Hanning window was applied to the time series and the frequency resolution was 8.79 Hz. The FFT block size was 2048, and using an overlap of 50%, the number of averages in the FFT was 61. From the FFT, at least four acoustic modes were present. The first and fourth modes were weak and in many occasions difficult to detect. The second and third modes were the dominant acoustic tones for this cavity L/D ratio and large amplitude peaks were observed. Figure 5 shows the variation of the frequencies of the first three modes with yaw angle. The solid lines are at $M = 1.11$, and the symbols are at $M = 0.84$. The nondimensional frequency is determined from the following expression:

$$St_n = \frac{f_n L}{U} = \frac{(n-\alpha)}{M[1+(\gamma-1/2)M^2]^{-1/2} + 1/k} \tag{1}$$

which is a modified form of Rossiter's [7] semi-empirical formula derived by Heller et al. [14] with the cavity speed of sound replaced by the freestream stagnation sound speed. In Eq. (1), n is the mode number, M the freestream Mach number, and the constants α and k were given by Rossiter for a cavity of $L/D = 4$ as 0.25 and 0.57, respectively.

Using Eq. (1), the frequencies at $\psi = 0$ deg are as follows: St= 0.29, 0.69, and 1.08 for modes 1, 2, and 3 at $M = 0.84$; $St = 0.27$, 0.64, and 1.0 for modes 1, 2, and 3 at $M = 1.11$. The experimental values at $\psi = 0$ deg are reasonably close to the theoretical values. The variation in frequency with ψ is not large, but the trend is toward a small increase for modes 1 and 2 and a decrease for mode 3. Up to the highest value $\psi = 20$ deg carried out in this investigation, the acoustic modes are excited in the longitudinal direction inside the cavity.

The amplitude of the nondimensional acoustic pressure along the cavity floor for the second and third modes at $M = 1.11$ is shown in Figs. 6 and 7. The amplitude of mode 2 in Fig. 6 is seen to increase to a maximum at $\psi = 5$ deg and thereafter decreases with increasing values of ψ. The modal amplitude drops rapidly from $\psi = 10$ to 15 deg when the aft wall is completely under the influence of the separating sidewall shear layer. The amplitude at $\psi = 20$ deg is fairly small and at some locations on the cavity floor the mode is difficult to detect.

The behavior of the amplitude is perplexing, as it is expected that, at $\psi = 0$ deg, the shear layer separating from the front edge will have traveled the full cavity length L and will have rolled up to form vortices. The excitation pressure forces at the corner of the aft wall will be larger than those at the larger values of ψ and, hence, the acoustic tones will be the strongest at $\psi = 0$ deg. In the next section, the pressure on the aft wall is investigated and this behavior is related to the flow at the aft wall, which affects the acoustic wave generation.

Figure 7 shows the amplitude of the acoustic wave mode 3. Increasing the yaw angle to $\psi = 5$ and 10 deg results in a decrease in amplitude throughout the length of the cavity floor. However, at

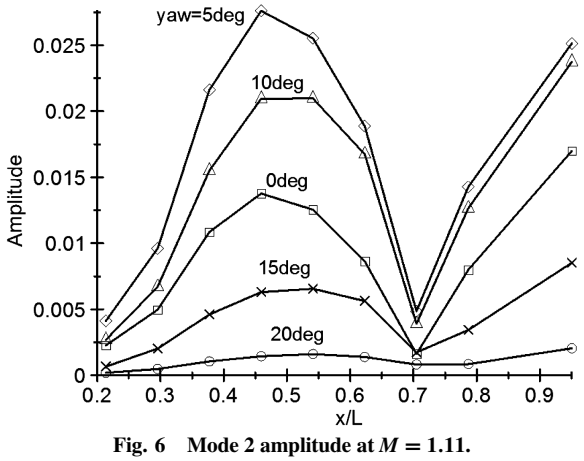

Fig. 6 Mode 2 amplitude at $M = 1.11$.

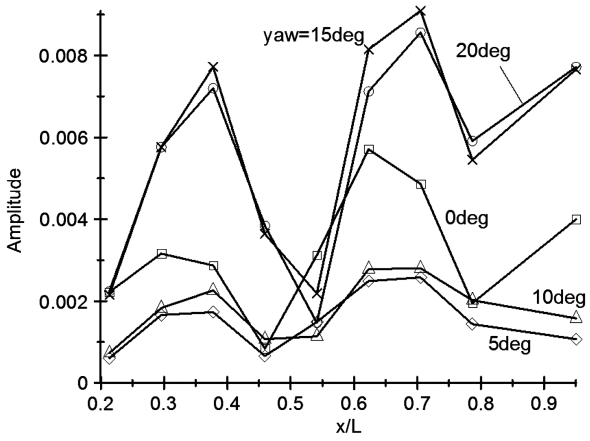

Fig. 7 Mode 3 amplitude at $M = 1.11$.

$\psi = 15$ and 20 deg, when the aft wall is completely under the influence of the separating sidewall shear layer, the mode amplitude increases above those at $\psi = 0$ deg. Comparing Fig. 6 with Fig. 7, it is seen that mode 2 is dominant over mode 3 until ψ reaches 15 deg when mode 3 becomes the dominant mode.

The variation of the amplitude of the second and third modes with x/L at $M = 0.84$ is shown in Figs. 8 and 9. Unlike the supersonic flow case, the amplitude of mode 2 is seen to be largest at $\psi = 0$ deg and decreases with increasing ψ. For mode 3, the amplitude does not vary significantly from the unyawed case until $\psi = 15$ deg, where a large increase is detected, and increasing ψ to 20 deg causes a reduction in modal amplitude from that at $\psi = 15$ deg. Similar to the results at $M = 1.11$, mode 2 is dominant until $\psi = 15$ deg when a switch over to mode 3 is detected.

Mode shapes are also given by Tracy and Plentovich [6]. At $M = 0.8$ and for a cavity with $L/D = 4.4$ and $L/W = 4.5$, which are close to the present cavity L/D and L/W ratios of 5, their results showed a lower amplitude for mode 2 by as much as 10 dB in terms of the sound pressure level when ψ increased from 0 to 15 deg. Mode 3 results were not shown. Increasing the Mach number to 0.9 showed the modal amplitude to be quite close together for ψ at 0 and 15 deg.

To obtain phase relationships, a cross-spectral analysis was carried out using transducer 11 as a reference. Some phase angles were difficult to measure due to the presence of noise. In the analysis, one block of data consisting of 63,488 samples was used. There were transducer locations on the cavity floor where the measured phase angles were not deemed to be reliable and the results were discarded. Figures 10 and 11 show the phase variation for mode 2 and mode 3, at $M = 0.84$ and 1.11. The angles were computed relative to that at transducer 11 located at $x/L = 0.786$, and the phase angle at transducer 11 was arbitrarily set to 0 deg. Figures 6 and 8 show that an amplitude minimum at approximately $x/L = 0.7$ occurs for both Mach numbers and all yaw angles. The phase curve in Fig. 10 shows a jump between 150 and 200 deg at this location on the cavity floor.

For mode 3, Figs. 7 and 9 show there are two minima between the two amplitude peaks at about $x/L = 0.5$ and 0.8. These values vary slightly with Mach numbers and yaw angles. Although there is no definite observable trend, the scatter is most likely due to measurement error. The spacing of the transducers on the cavity floor did not have sufficient spatial resolution for accurate measurements of the two minima. Figure 11 shows a phase shift between 120 and 160 deg at approximately $x/L = 0.5$. The $M = 1.11$ curve at $\psi = 0$ deg does not represent the position of the jump with sufficient accuracy because the phase measurements at transducer 7 ($x/L = 0.459$) were corrupted by noise and no data were available at

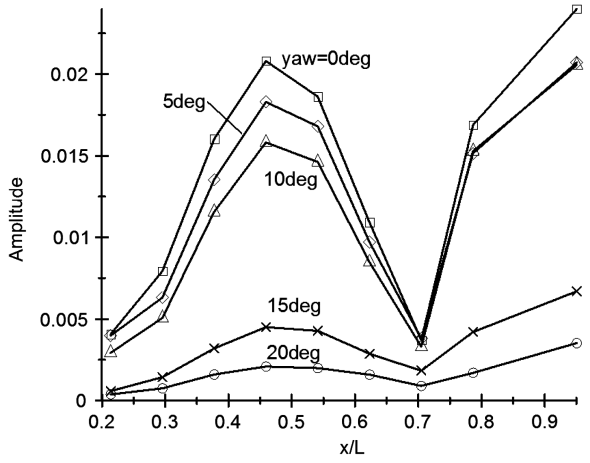

Fig. 8 Mode 2 amplitude at $M = 0.84$.

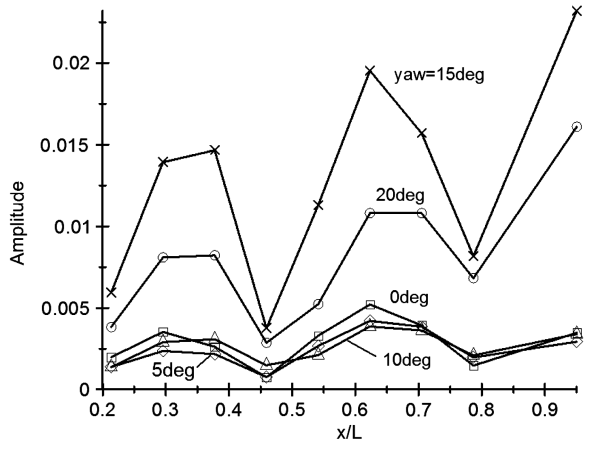

Fig. 9 Mode 3 amplitude at $M = 0.84$.

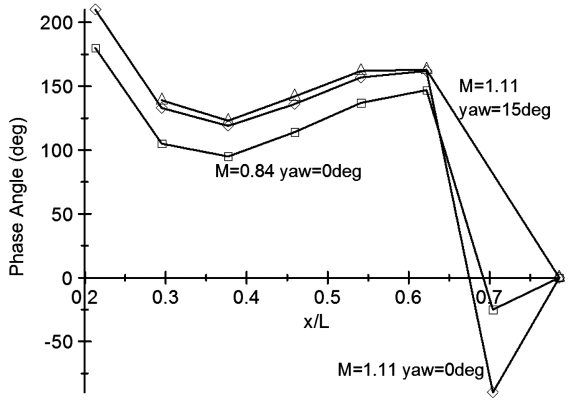

Fig. 10 Mode 2 phase angle at $M = 0.84$ and $M = 1.11$.

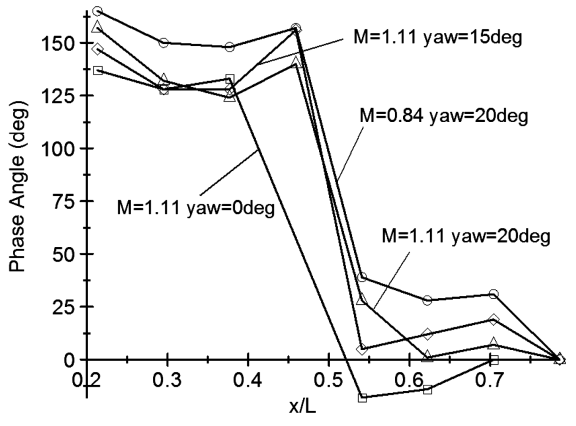

Fig. 11 Mode 3 phase angle at $M = 0.84$ and $M = 1.11$.

that location. Closer transducer spacing is required to give more accurate phase measurements. There were insufficient transducers installed at the rear of the cavity to determine whether there was a phase shift at $x/L = 0.8$.

IV. Wall Pressure Measurements

A. Aft Wall C_p and $C_{p_{\text{rms}}}$

Three transducers were available on the aft wall for unsteady pressure measurements. Transducers 14, 15, and 16 (see Fig. 1) were located at $y/D = 0.752$, 0.501, and 0.268, respectively. The spatial resolution was not sufficiently high to provide accurate data to show the details of the pressure variations on the aft wall. However, some indications of the effect of yaw on the pressure and generation of acoustic waves can be deduced from the limited data.

Figure 12 shows the time-averaged pressure coefficient C_p on the aft wall at $M = 1.11$. The pressure on the cavity floor at $x/L = 0.95$ is also included for comparison purposes. The measurements do not represent the pressure at the base of the cavity ($y/D = 1$), but only serve to give an idea of the pressure in that vicinity. At transducer 16, closest to the upper corner of the cavity, the pressure decreases rapidly with ψ. Deeper inside the cavity, transducers 15 and 14 show the pressure to increase with ψ until $\psi = 10$ deg before it starts to decrease. The pressure measured by transducer 13 located on the cavity floor follows the trend of transducer 14.

For the unyawed cavity, C_p drops from about 0.24 to 0.16 from $y/D = 0.268$ to 0.752. Some aft wall pressure measurements by Stallings and Wilcox [15] for an open cavity with $L/D = 4$ at supersonic Mach numbers showed the pressure gradient on the aft wall to be large and C_p decreased until y/D reached a value of approximately 0.75 before it started to increase. The trend was similar for all transitional flows they investigated and the minimum pressure was found to occur from between $y/D = 0.5$ to 0.75 for the Mach numbers and L/D ratios they investigated. In Fig. 12, it is seen that C_p increases instead of decreasing with y/D for $\psi \geq 5$ deg. Transducer 14, closest to the cavity floor, has the highest pressure for $\psi > 5$ deg. In Fig. 3, it is observed that the C_p distribution along the cavity floor shows a transitional-open flow behavior. The C_p distribution on the aft wall for $\psi \geq 5$ deg bears no resemblance to those for transitional-open cavities obtained by Stallings and Wilcox [15]. It is not surprising that the aft wall C_p distribution behaves differently because the flow inside the yawed cavity differs from that inside transitional-open cavities at $\psi = 0$ deg investigated by Stallings and Wilcox [15]. The differences can be observed from the numerical computations obtained by Baysal and Yen [4].

Figure 13 shows the C_p distribution on the aft wall at $M = 0.84$. The pressure measured at $y/D = 0.268$ from transducer 16 decreases very slightly with increasing ψ until $\psi = 15$ deg. Further increase to

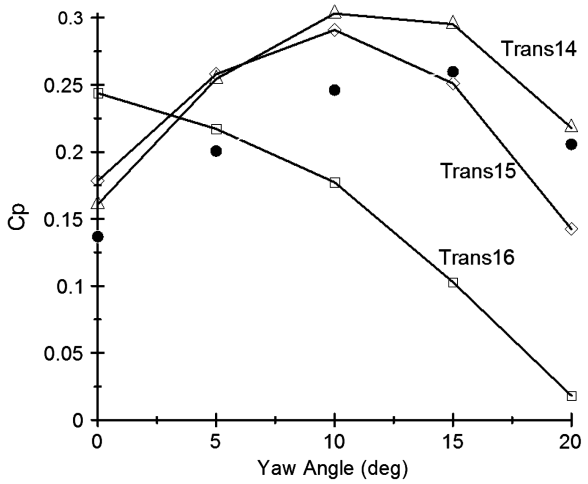

Fig. 12 C_p distribution on aft wall at $M = 1.11$. Filled circle: C_p on cavity floor at $x/L = 0.95$.

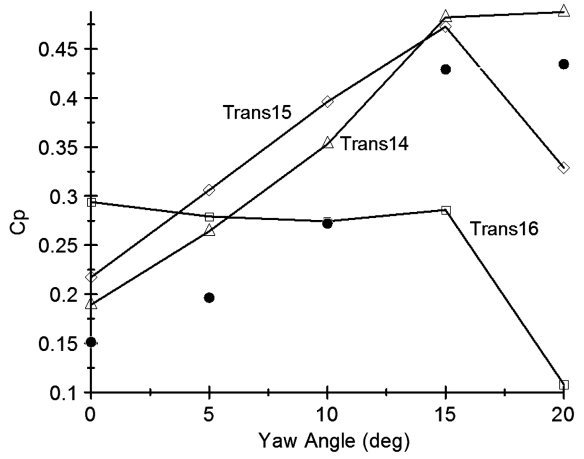

Fig. 13 C_p distribution on aft wall at $M = 0.84$. Filled circle: C_p on cavity floor at $x/L = 0.95$.

$\psi = 20$ deg results in a rapid drop to a lower value. On the other hand, transducers 14 and 15 measured pressure that increases until ψ reaches 15 deg. At this yaw angle, the pressure closer to the floor ($y/D = 0.752$) remains fairly constant, whereas the pressure at $y/D = 0.501$ decreases. The floor pressure at $x/L = 0.95$ follows the pressure trend measured by transducer 14. At $\psi = 0$ deg, the pressure distribution decreases toward the cavity floor, but at $\psi \geq 5$ deg, the pressure increases with cavity depth. The pressure maximum at $y/D = 0.501$ occurs only for ψ between 5 and 10 deg.

Plentovich et al. [16] measured the aft wall pressure at subsonic and transonic Mach numbers for a variety of L/D ratios covering open, transitional, and closed flows. They found that, for an open cavity, the peak pressure on the aft wall occurred nearest to the edge of the aft wall corner. For a closed cavity, the peak pressure occurred at a certain distance down the cavity edge, and, for transitional flows, the peak occurred at a distance just off the top of the aft wall similar to the closed flow. In all the cases they investigated, the pressure dropped from the maximum to the base of the cavity. The measurements from Plentovich et al. [16] were limited to four locations on the aft wall. Henderson et al. [17] carried out CFD computations and obtained detailed aft wall pressure distributions. Their results agreed with the trend obtained from the experiments carried out by Plentovich et al. [16]. The present results for a yawed cavity do not agree with the transitional flow aft wall pressure results obtained by Plentovich et al. [16], Henderson et al. [17], and Stallings and Wilcox [15] for an unyawed cavity in both transonic and supersonic flows. This suggests that the shape of the C_p curves on the cavity floor, such as those shown in Fig. 3, cannot be used to classify the flow for a yawed cavity as being transitional or transitional-open. The flowfield bears no resemblance to those given by Plentovich et al. [5], which are based on L/D ratios.

The $C_{p_{\text{rms}}}$ on the aft wall at $M = 1.11$ and $M = 0.84$ is shown in Figs. 14 and 15. In Fig. 14, the pressure fluctuations are largest at transducer 16, which is closest to the cavity edge and the fluctuations decrease toward the cavity floor. When $\psi > 10$ deg, the unsteady pressure decreases rapidly with increasing ψ and the variations between transducers are small. The $C_{p_{\text{rms}}}$ on the cavity floor at $x/L = 0.95$ remains small compared to the aft wall values, except for the highest ψ case when they are all fairly close together.

The results at $M = 0.84$ shown in Fig. 15 are quite similar to those for $M = 1.11$ with the exception that the sharp decrease in $C_{p_{\text{rms}}}$ closest to the floor (transducer 14) begins at $\psi = 15$ deg.

B. Mode Amplitude and Phase

The amplitudes of mode 2 and 3 for $M = 1.11$ are shown in Fig. 16 for the three aft wall transducers. The variations in the magnitude between transducers are small. Mode 2 is dominant up to a value of ψ very close to 15 deg. The two modes are of equal strength at $\psi = 15$ deg and, above this yaw angle, the third mode is dominant. However, the amplitudes are small for both modes when

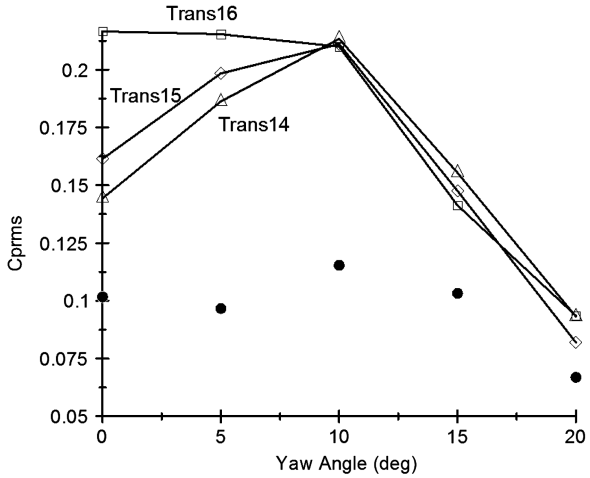

Fig. 14 C_{prms} distribution on aft wall at $M = 1.11$. Filled circle: C_{prms} on cavity floor at $x/L = 0.95$.

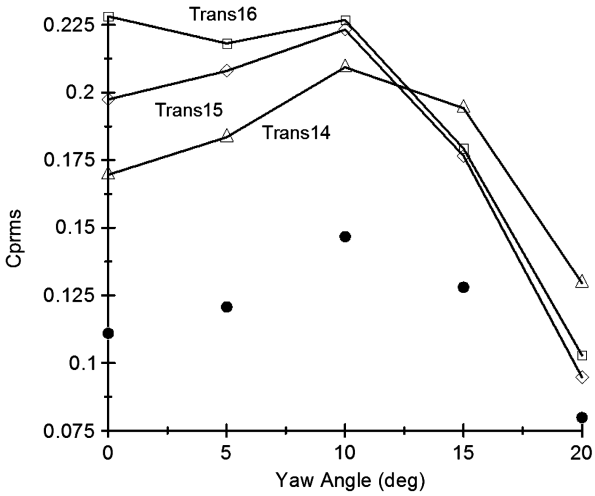

Fig. 15 C_{prms} distribution on aft wall at $M = 0.84$. Filled circle: C_{prms} on cavity floor at $x/L = 0.95$.

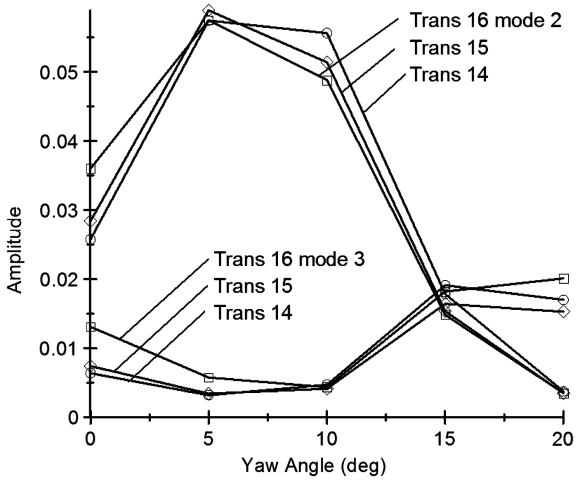

Fig. 16 Mode amplitude on aft wall at $M = 1.11$.

$\psi \geq 15$ deg. It is seen from this figure that mode 2 increases in amplitude above the unyawed value up to $\psi = 10$ deg with the highest value at $\psi = 5$ deg. Beyond this angle, the amplitude decreases. This is in agreement with the amplitude curves given in

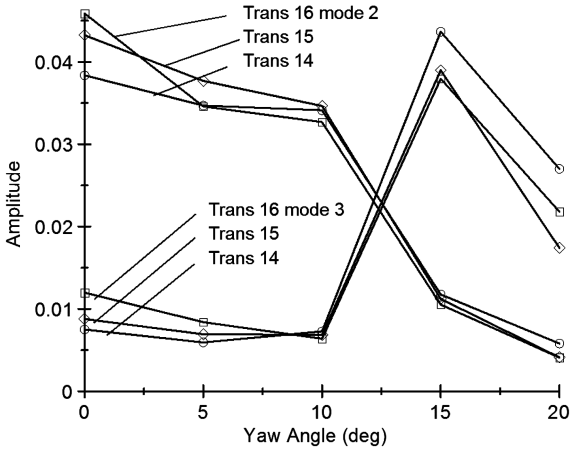

Fig. 17 Mode amplitude on aft wall at $M = 0.84$.

Fig. 6 which shows the amplitude of mode 2 at $\psi = 5$ deg to have the highest value before it starts to decrease with increasing ψ.

The mode amplitudes on the aft wall at $M = 0.84$ are shown in Fig. 17. Mode 2 decreases from $\psi = 0$ to 10 deg gradually before a steep drop to $\psi = 20$ deg. Mode 3, on the other hand, starts to increase at $\psi = 10$ deg and reaches a maximum at $\psi = 15$ deg before it decreases sharply to a lower amplitude at $\psi = 20$ deg. For $\psi \geq 15$ deg, mode 3 is the dominant mode. This is in agreement with the results shown in Figs. 8 and 9.

It is informative to know the phase relationship of the pressure measured from the three transducers on the aft wall. As in the previous section on phase measurements along the cavity floor, a cross-spectral analysis was carried out with one data block consisting of 63,488 samples and having transducer 16 as the reference signal. The phase difference between transducers 15 and 14 was computed. Because of the lack of transducers on the aft wall, phase angles were only available showing the phase shift in modes 2 and 3 between $y/D = 0.501$ and 0.752. The spatial separation for the two measurement points is approximately one-fourth of the cavity depth.

Figure 18 shows the phase shift between the two modes in the range of ψ where they are dominant for $M = 0.84$ and 1.11. The results show that, for the unyawed cavity, the phase difference is small, but it increases with ψ. The effect of Mach number is large for the third mode. A large phase shift suggests that pressure waves generated on the aft wall are not planar.

C. Front Wall Pressure and Mode Measurements

The pressure on the front wall measured by transducer 1 located at $y/D = 0.626$ is shown in Fig. 19. The transducer is located in a quiescent region although the flow is quite complex because of the

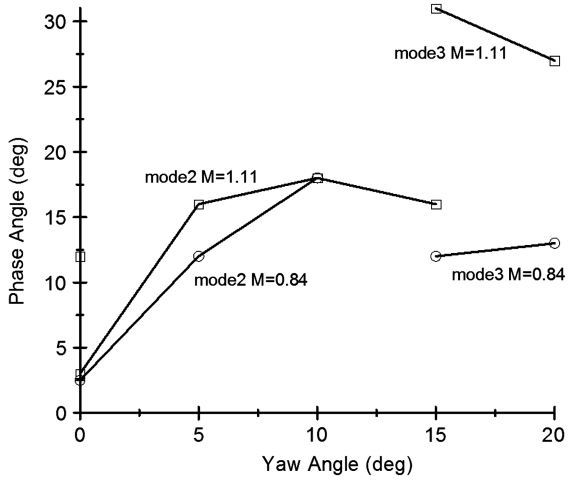

Fig. 18 Phase angle of modes 2 and 3 on aft wall.

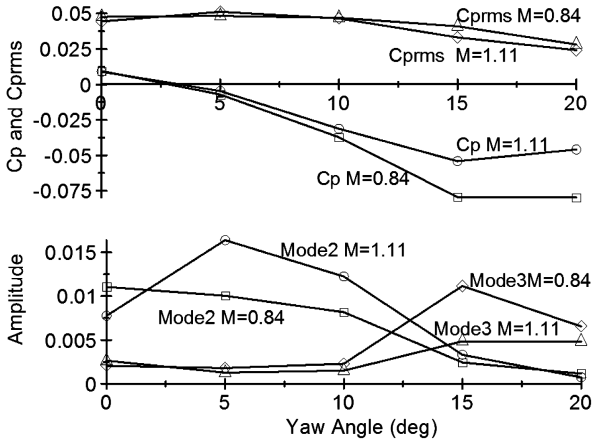

Fig. 19 Pressure and mode amplitude on front wall.

presence of a recirculating vortex and additional secondary vortices [18]. Negative pressure develops at $\psi \geq 5$ deg as shown in the cavity floor C_p distribution (Fig. 3). The $C_{p_{\text{rms}}}$ is small compared to that at the aft wall and it varies only slightly with ψ. The amplitudes of modes 2 and 3 are also small and the switch over from mode 2 to mode 3 with ψ is consistent with Figs. 16 and 17.

V. Conclusions

Rossiter's [7] empirical formula was found to give good estimates of the resonant frequencies for moderate yaw angles up to 20 deg, which was the highest value tested. The amplitude of the acoustic wave was a function of the yaw angle. The dominant mode switched over to a higher mode when the yaw angle exceeded a critical value that was dependent on the dimensions of the cavity. For a cavity with L/D and L/W ratios of 5, mode 2 was the dominant mode and the switch over to mode 3 occurred when the yaw angle was approximately 15 deg. Phase measurements on the cavity floor detected a phase shift in the vicinity of 180 deg near the first minimum in the mode shape curves. At $M = 0.84$ and $M = 1.11$, the aft wall pressure distributions and acoustic mode amplitudes showed a very different behavior with changes in yaw angle for transonic and supersonic flows.

References

[1] Komerath, N. M., Ahuja, K. K., and Chambers, F. W., "Prediction and Measurement of Flows Over Cavities: A Survey," AIAA Paper 87-1066, Jan. 1987.

[2] Chokani, N., "Flow Induced Oscillations in Cavities: A Critical Survey," AIAA Paper 92-02-159, May 1992.

[3] Grace, S. M., "An Overview of Computational Aeroacoustics Techniques Applied to Cavity Noise Prediction," AIAA Paper 2001-0510, Jan. 2001.

[4] Baysal, O., and Yen, G. W., "Implicit and Explicit Computations of Flows past Cavities with and Without Yaw," AIAA Paper 90-0049, Jan. 1990.

[5] Plentovich, E. B., Chu, J., and Tracy, M. B., "Effects of Yaw Angle and Reynolds Number on Rectangular-Box Cavities at Subsonic and Transonic Speeds," NASA TP 3099, April 1991.

[6] Tracy, M. B., and Plentovich, E. B., "Characterization of Cavity Flow Fields Using Pressure Data Obtained in the Langley 0.3-Meter Transonic Cryogenic Tunnel," NASA TM 4436, Feb. 1993.

[7] Rossiter, J., "Wind-Tunnel Experiments on the Flow over Rectangular Cavities at Subsonic and Transonic Speeds", Aeronautical Research Council Rept. and Memo. 3438, Great Britain, Oct. 1964.

[8] Bilanin, A. J., and Covert, E. E., "Estimation of Possible Excitation Frequencies for Shallow Rectangular Cavities," *AIAA Journal*, Vol. 11, No. 3, 1973, pp. 347–351. doi:10.2514/3.6747

[9] Tam, C. W. W., and Block, P. J. W., "On the Tones and Pressure Oscillations Induced by Flow over Rectangular Cavities," *Journal of Fluid Mechanics*, Vol. 89, Pt. 2, 1978, pp. 373–399. doi:10.1017/S0022112078002657

[10] Heller, H., and Bliss, D., "Aerodynamically Induced Pressure Oscillations in Cavities: Physical Mechanisms and Suppression Concepts," U.S. Air Force Flight Dynamics Lab. TR-74-133, Feb. 1975.

[11] Henshaw, M. J. de C., "M219 Cavity Case," *Verification and Validation Data for Computational Unsteady Aerodynamics*, Research and Technology Organization TR-26, Oct. 2000.

[12] Orchard, D. M., Lee, B. H. K., and Tang, F. C., "Influence of Captive Stores on the Unsteady Pressure Distribution Within a Rectangular Cavity," International Council of the Aeronautical Sciences Paper 2006-3.9.4.,Sept. 2006.

[13] Lee, B. H. K., "Analysis of Data on the Effect of Yaw on the Flow Inside a Rectangular Cavity," National Research Council Canada NRC CR-678158, Oct. 2008.

[14] Heller, H. H., Holmes, D. G., and Covert, E. E., "Flow-Induced Pressure Oscillations in Shallow Cavities," *Journal of Sound and Vibration*, Vol. 18, No. 4, 1971, pp. 545–553. doi:10.1016/0022-460X(71)90105-2

[15] Stallings, R. L., Jr., and Wilcox, F. J., Jr., "Experimental Cavity Pressure Distributions at Supersonic Speeds," NASA TP 2683, March 1987.

[16] Plentovich, E. B., Stallings, R. L., Jr., and Tracy, M. B., "Experimental Cavity Pressure Measurements at Subsonic and Transonic Speeds," NASA TP 3358, July 1993.

[17] Henderson, J., Badcock, K., and Richards, B. E., "Subsonic and Transonic Transitional Cavity Flows," AIAA Paper 2000-1966, June 2000.

[18] Torda, T. P., and Patel, B. R., "Investigations of Flow in Triangular Cavities," *AIAA Journal*, Vol. 7, No. 12, 1969, pp. 2365–2367. doi:10.2514/3.5555